Drop Sizes and Mass Fluxes Development in a Pressure Swirl Hollow Cone Spray

J.L. Santolaya, L.A. Aísa, J.A. García, I. García Palacín, E. Calvo.
e-mail: laisa@posta.unizar.es

Fluid Mechanics Area. Zaragoza University, María de Luna, 3,
50015 - Zaragoza (SPAIN), Phone: (34) 976-761881; Fax: (34) 976-761882

Abstract

An experimental study of a wasted oil spray generated by a pressure swirl atomizer type has been carried out, based mainly on measurements performed by means of a PDA system. The injection pressure range covers two spray regimes: (I) Sheet breakup by perforations; (II) Sheet breakup in border by surface waves instability.
Emphasis has been made in the analysis of drop sizes and flux development in addition to integral flow rate evaluation in many transversal sections. The axisymmetrical surface that contains a 50% of the cumulated flow rate has been used as reference at each section and it allows us to describe the spray structure and dispersion characteristics.
The axial evolution of flow rates by size class has been compared with results obtained by means of a simple model of droplet collision. A coalescence efficiency of 100% has been supposed. Results agree qualitatively with measurements taken in a suitable spray region but the calculated diameter distribution is far from the measured one.

1. Introduction

The operation of pressure swirl nozzles, frequently used in combustion systems, is based on the high liquid swirl inside the injector that results in a liquid conical sheet at the exit. The sheet disintegrates at some distance of the exit because of different breakup mechanisms. The fluid properties, the injection conditions and the geometry of the atomizers establish the characteristics of the discharge flow and the development and disintegration of the liquid sheet.
The hollow cone spray structure is conditioned by the breakup sheet mechanisms. The right size and spatial droplet distribution are conclusive for combustion and other applications, and they depend on different physical phenomena. When the secondary drop disintegration and evaporation are negligible, droplet collision phenomena, as well as the dispersion and mixing dynamics, rule drop sizes evolution and liquid distribution [2, 3, 4]. The study of collisions and the development of models have been the main subjects of many works [5, 6].
The present work deals with the structure of a wasted oil spray generated by a pressure swirl nozzle (PSN). Measurements of droplet size distribution, flux and concentration have been performed with PDA techniques correcting the effective probe volume dimensions [1].
The volume size distribution of droplets has been obtained by integration of the local flux over the whole cross section. Streamwise change has been compared with the results obtained by means of a simplified model of droplet collision. This model assumes that all collisions end in a coalescence.

2. Experimental setup

Fig.1), shows the experimental setup used in this research. The main purposes were to generate a spray under controlled conditions and to provide optical access for the PDPA.
The injector is a hollow cone pressure swirl type with a liquid film cone angle of 80º and low flow rate. The liquid is wasted oil whose properties have been measured for the test conditions in laboratory, as table 1 shows.
The facility can set the following injection pressure and temperature ranges, 0-24 bar and 20º-95ºC. In these experiments, the temperature has been constant and three pressures have been set. Table 2 shows injection conditions. The oil has been injected into a square section chamber where a low velocity co-flow surrounds the spray.
A low noise camera CCD and a stroboscopic light source have been used to visualize the sheet disintegration. A PDPA system of TSI-Aerometrics with simultaneous acquisition of size and two components of velocity has been employed to characterize the spray. The reception optics was placed at 70º from the beams' plane, and both emitter and receiver were mounted onto a three-dimensional traversing system.
For each pressure, spray data have been obtained in a set of points located at four transversal sections, s_0, s_1, s_2, s_3, at axial distances x=9, 18, 36, 72 mm from the exit.

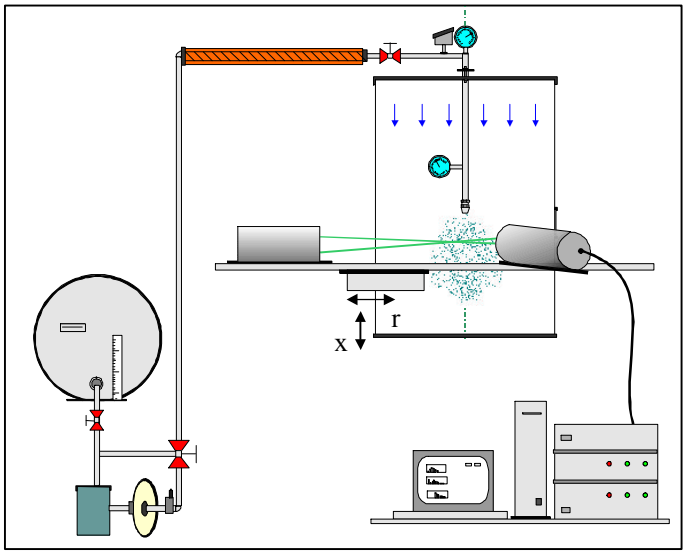

Figure 1.Experimental setup.

Table 1. Oil Properties.

	r (Kg/m^3)	n (m^2/s)	s (N/m)
T = 95º C, P = 12÷20 bar	850	$16 \cdot 10^{-6}$	0.032
	Refraction index: **m** = 1.483 + 0.00072i		

Table 2. Test conditions.

T = 95º C	**P=12 bar**	Q=0,662 ml/s
	P=16 bar	Q=0,777 ml/s
	P=20 bar	Q=0,854 ml/s

3. Flow structure

The flow at the atomizer exit forms a conical sheet, whose disintegration is illustrated in the photographs of the figure 2) for each injection pressure. Increasing pressure generates big differences in the length sheet and in the breakup mechanisms, and it is possible to define two distinct regimes. For regime I, with P=12 bar, superficial waves together with film holes and highly developed sheets appear. For higher pressures, P=16 and P=20 bar, only surface waves cause the sheet disintegration in locations near the atomizer exit (regime II).

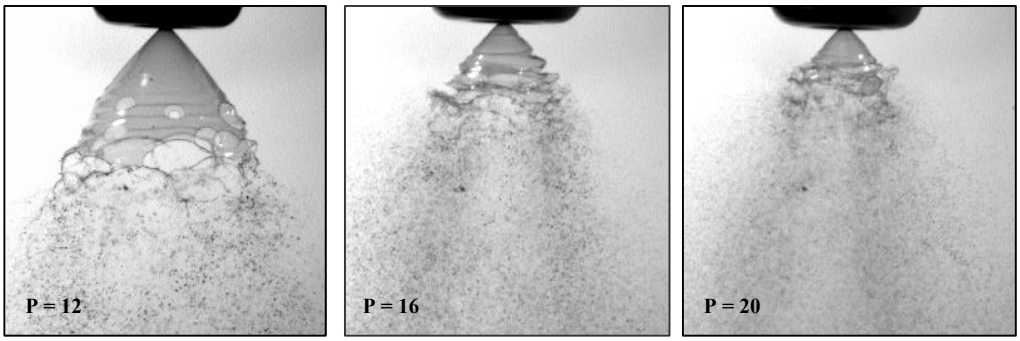

Figure 2. Sheet disintegration images.

The initial conditions determine the later structure of the spray, as it can be seen in the evolution of the parameter R50 (figure 3). This parameter is the radial position that includes 50% of the volume flow measured in the section, and it was used in this experiment to generate the dimensionless radial coordinate defined as r*=r/R50. In a similar way, the radii R90 and R10, which include 90% and 10% of the flow in each section, have been defined.
The figure 3) also shows the cumulated flow rate (defined as the axial flux integrated over a circular cross-section of radius "r") for the case of P=16 bar, under hypothesis of axis-symmetry. It shows a flow deficit in the first section due to measurement troubles generated by the high concentration of drops. At more advanced sections, measured total flow rate is nearly constant. R50 parameter increases for downstream sections, because of the conical structure of the flow. In the test pressure range, its evolution is related to the two types of sheet development and breakup previously pointed. On going from P=12 to P=16, R50 increases, and then, for P=20, it reduces again.

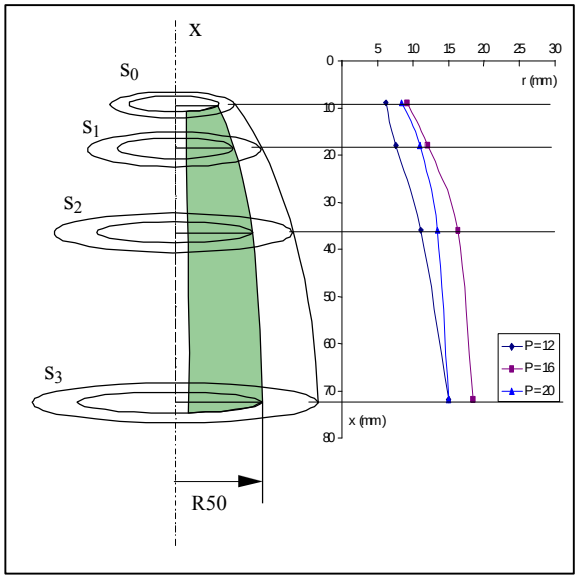

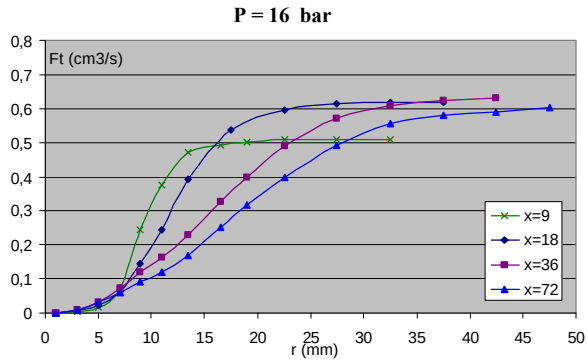

R50	P = 12	P = 16	P = 20
x = 9	6,21	9,13	8,40
x = 18	7,59	12,11	11
x = 36	11,14	16,31	13,46
x = 72	15,02	18,49	15,04

Figure 3. Flow rate measured in P=16 bar. R50 evolution for the tree injection pressure.

In figures 4-a) and 4-b), measurements of mean axial velocity profiles for all droplets, and Sauter diameter profiles of the local size distributions, are presented. The profiles are plotted with r* value of each section and for the three injection pressures. For P=12 bar, axial velocity profiles reach maximum values in the region near the breakup point. If the pressure increases (P=16, 20 bar) a spray with Vx maximum at the central region is generated. In addition, these profiles show a flat zone around r* = 1 for the exit sections near to the nozzle.

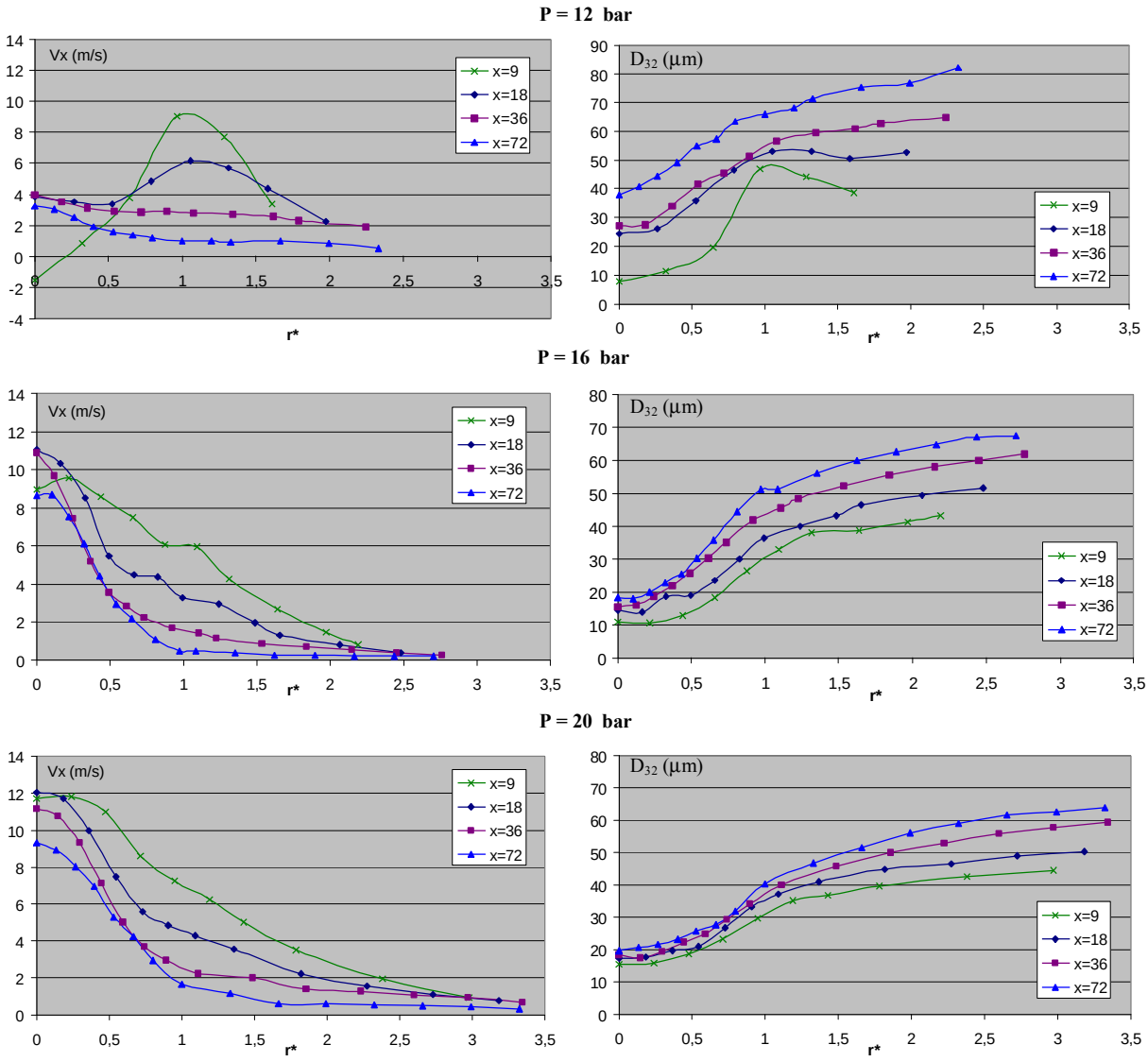

Figure 4-a.
Axial mean velocity profiles.

Figure 4-b.
Sauter mean diameter profiles.

Sauter diameter increases progressively towards the spray border due to the inertial classification of the droplet size distribution, the aerodynamic drag of droplets and other phenomena. In general, the higher injection pressures, the smaller D_{32} was obtained and radial profiles evolve more slowly in downstream sections than for the previous case.

In the figures 5-a) and 5-b), the axial flux profiles (F_v) and percentage of cumulated axial flow rate (%Ft) are plotted versus r*, which has been obtained for each test pressure.

Flux profiles show a well-defined maximum at the exit sections near to the nozzle due to the hollow cone sheet shape. This profile type is especially outstanding for low injection pressures, where more developed sheets have been observed.

A progressive reduction of maximum value of flux and the broadening of the spray happen in farther sections and for each pressure. A dispersion parameter is defined from the graphs of accumulated axial flow rate as $\Delta R^*=R90^*-R10^*$. It grows with the axial coordinate because of droplet flow rate redistribution.

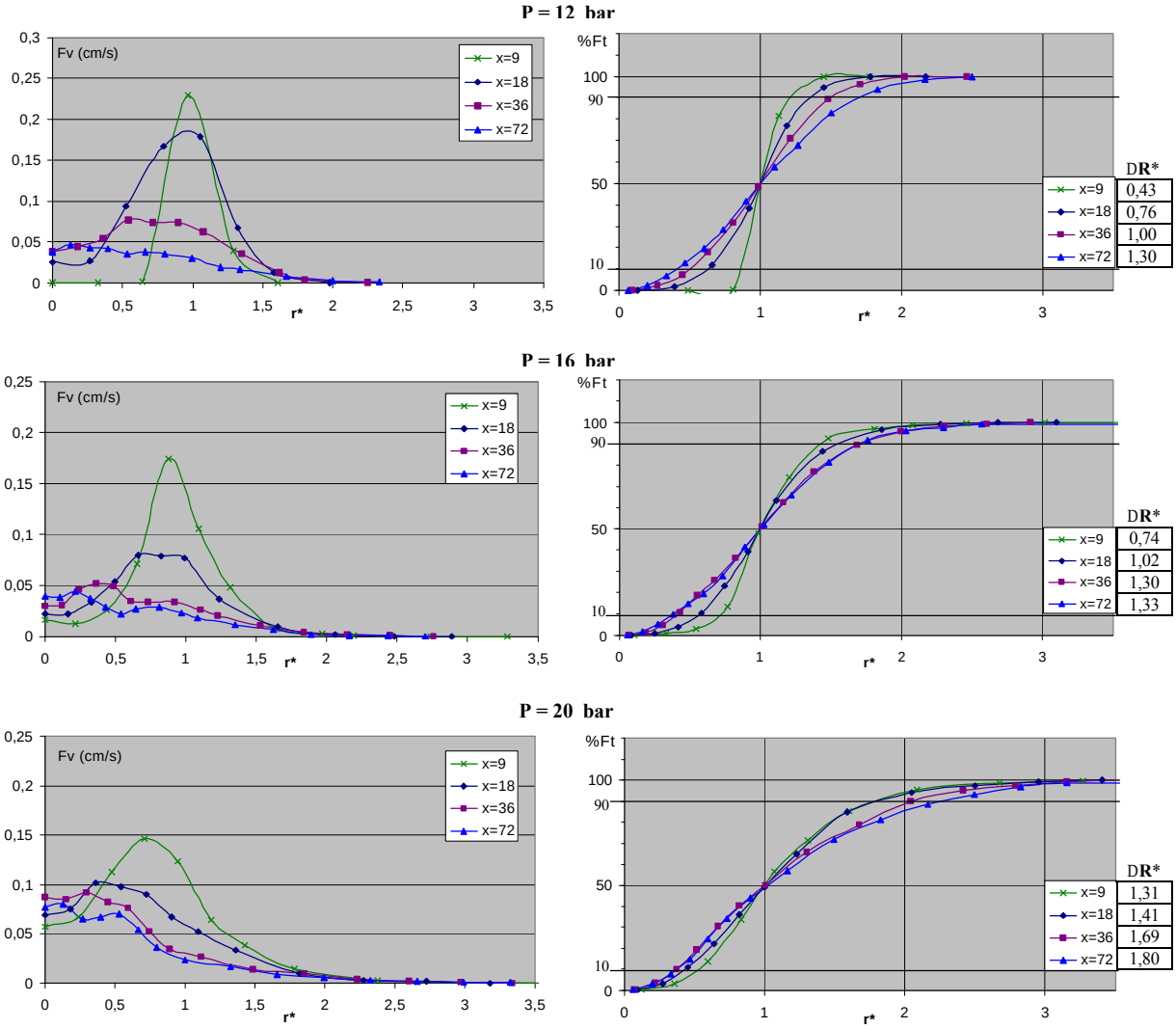

Figure 5-a. Axial flux profiles.

Figure 5-b. Cumulated axial flow rate.

Axial evolution of droplet flux shows a distinctive behavior for each size class. In the figure 6), axial flux profiles of the size classes (5-10), small, (20-30), medium and (50-60) large, have been plotted for the case P=16 bar. The comparison between two sections, located at 9 and 36 mm from the exit, shows that maximum axial flux value of the small size class is found at the central zone, while the large size class has an axial flux maximum value at the external radial locations, which moves approaching the border of the spray.

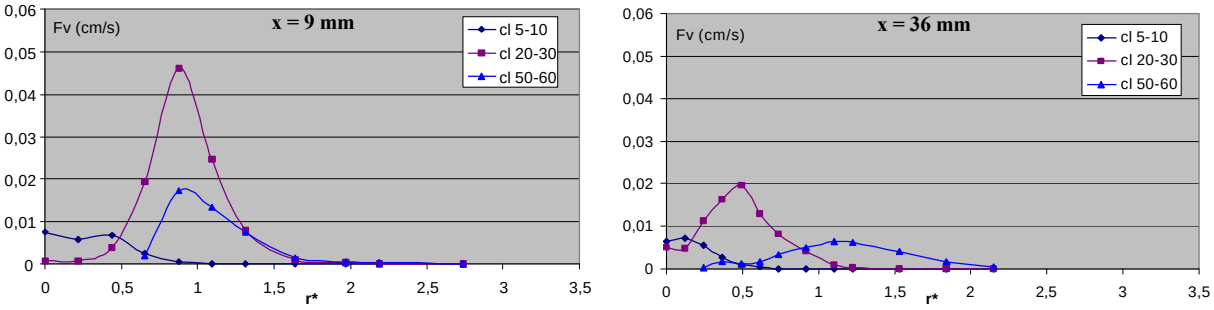

Figure 6. Axial flux profiles by droplet size classes. P=16 bar.

4. Flow rate distribution by size classes. Comparison with a model

4.1 Flow rate distribution by size classes and cross section

Following, the flow rate percentage of every size class has been plotted in figure 7) for all three pressures at each cross section.

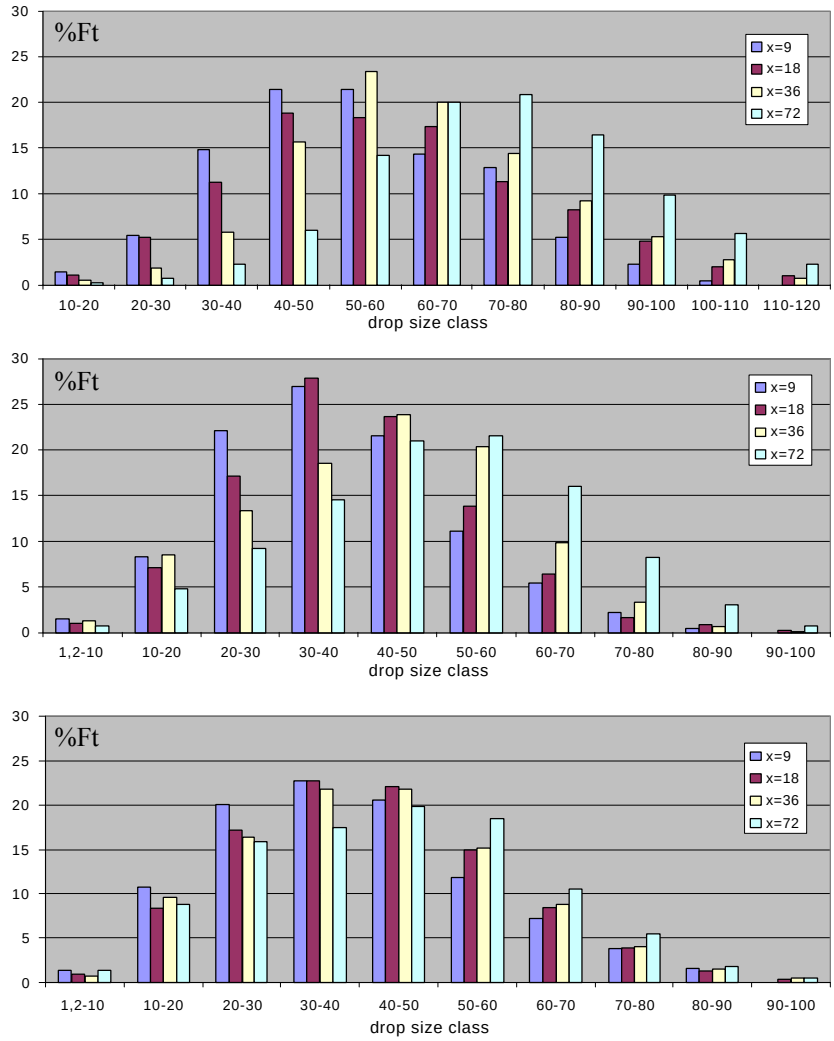

P = 12 bar

	D_m (mm)	s (mm)
x = 9	54,75	18,25
x = 18	59,14	20,90
x = 36	63,24	18,62
x = 72	73,63	19,24

P = 16 bar

	D_m (mm)	s (mm)
x = 9	37,89	14,92
x = 18	39,95	15,01
x = 36	42,71	16,30
x = 72	49,67	17,93

P = 20 bar

	D_m (mm)	s (mm)
x = 9	39,34	16,98
x = 18	41,49	16,69
x = 36	41,73	17,14
x = 72	43,47	18,07

Figure 7. Percentage of flow rate by droplet size classes and cross sections.

As a first conclusion, the percentage of large size classes flow rate grows up when the axial distance increases. The observed low droplet Weber number ($We_{max} < 1$) and the constant total flow rate ensures us that the drop coalescence is the cause of this size distribution deformation.

The tables next to the figure show the values of size distribution moments. For all pressures, there is an increase of mean diameter, D_m, more important for low injection pressures. It can be noticed that the sprays generated with P=16 bar and P=20 bar (regime II) have a quite smaller mean diameter than the one obtained by P=12 bar (regime I).

4.2 Comparison between measurements and a droplet collision model

A droplet collision model, based on kinetic theory of gases, has been used as a first step to analyze the coalescence effect [3].

According to this theory, the collision frequency of one droplet of diameter D_i with another D_j droplet size class can be calculated according to the expression:

$$f_c = \frac{\pi}{4}\left(D_i + D_j\right)^2 \mid \mathbf{u}_i - \mathbf{u}_j \mid n_j$$

D_i, D_j = Diameter of i^{th} and j^{th} size classes,
$\mathbf{u_i}$, $\mathbf{u_j}$ = Mean velocity vector of i^{th} and j^{th} size classes,
n_j = j^{th} class number concentration.

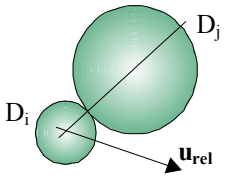

The following assumptions have been used for our calculations:
- The droplet number concentration is small enough that binary collision is dominant but it is high enough to allow a statistical treatment.
- A coalescence event happens for each collision.
- The mean size and velocity values have been assumed for each size class.

Under these conditions, we have calculated systematically the collision frequency that takes place for all couples of size classes. This evaluation has been applied to the stationary spray generated by an injection pressure of 16 bar. A region among sections s_1 and s_2 has been chosen because it presents a constant measured total flow rate and small droplet residence times (lower than 10^{-2} s).
Figures 8-a) and 8-b) show the axial velocity profiles of each droplet size class and the calculated collision frequencies for the 55 µm diameter class with other sizes at the section s_1, respectively.

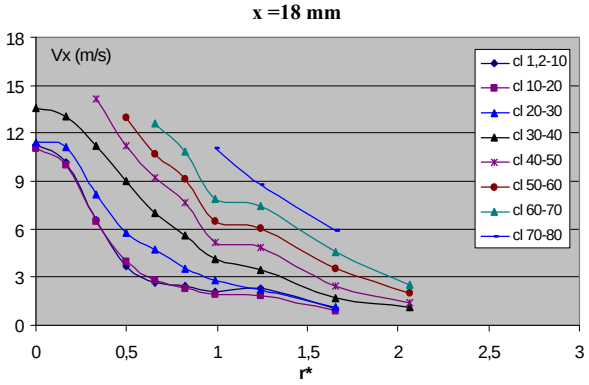

Figure 8-a. Axial mean velocity profiles by droplet size classes. P=16 bar.

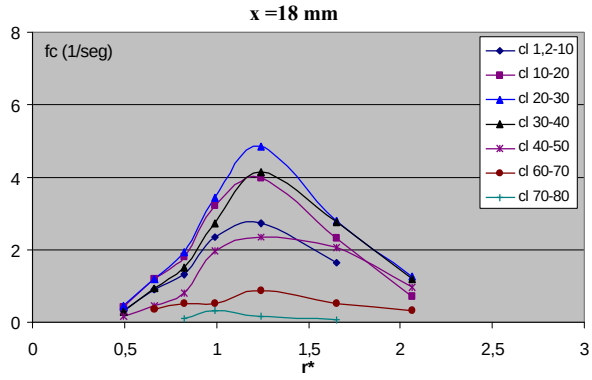

Figure 8-b. Collision frequency profiles for class 50-60. P=16 bar.

The size distribution evolution from s_1 to s_2 is evaluated afterwards. Two algorithms have been used. The first one supposes that the collision events take place with the flow properties of the section s_1. The second one splits the volume among sections in two parts of the same length. In the first volume, the properties measured in s_1 have been used and in the second these corresponding to s_2. Results with the second algorithm have been compared with the measured distribution in figure 9).
The final size distribution shape calculated at section s_2 agrees with the measured one but the numerical values do not match. This indicates the presence of other phenomena that play a decisive role in the droplet collision, therefore, making it necessary to improve the simple model used.

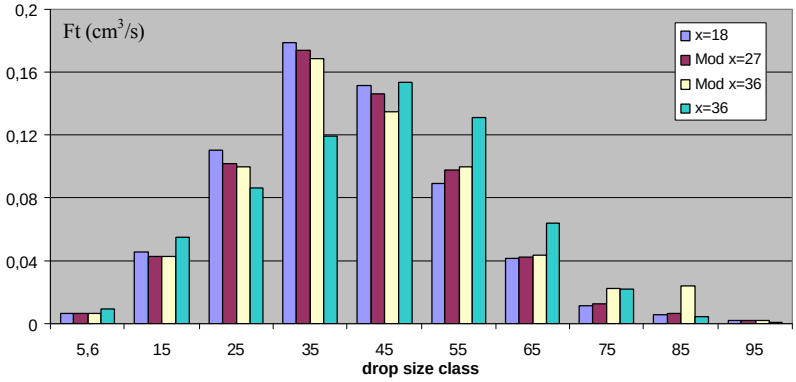

Figure 9. Droplet size distributions calculated with collision model.

5. Conclusions

The study of the spray structure generated by a PSN has been carried out for three injection pressures: 12, 16 and 20 bar.

Two different regimes have been recognized. Regime I, for P=12 bar, is characterized by a highly developed conical sheet. The film is broken due, mainly, to perforations and it results in a relatively coarse spray. The regime II, for P=16 and P=20 bar, is characterized by a short liquid sheet broken due to the growth of surface waves. This kind of disintegration produces a fine spray with an increased dispersion capacity.

Emphasis on the spray drop size development and the flux distribution has been made. Droplet mean diameter grows with the radius and it increases downstream.

The analysis of each size class flow rate shows a variation of the droplet size distribution toward the biggest size classes, in downstream sections. This fact together with the flow rate conservation allows us to assume the coalescence to be the main phenomenon responsible for this evolution.

A simplified model of collision, based on kinetic theory of gases, has been used to evaluate the change of the droplet size distribution in the steady flow. If the coalescence efficiency is equal to 100%, this model predicts a growth of the drop sizes, as confirmed by the measurements. However, the calculated diameter distribution evolution does not exactly match the measured one. In consequence, it would be necessary to improve the used model.

6. References

[1] L. Aísa, J.A. García, L.M. Cerecedo, I. García Palacín, E. Calvo., "Particle concentration and local mass flux measurements in two phase flows with PDA. Application to a study on the dispersion of spherical particles in a turbulent air jet". *International Journal of Multiphase Flow*, Vol 28, pp.301-324, 2002.

[2] J.L. Santolaya, L.A. Aísa, J.A. García, I. García Palacín, E. Calvo. "Dynamic characterisation of a pressure swirl hollow cone spray". ILASS 2002, Zaragoza, Spain, September 2002.

[3] M. Sommerfeld, G.Kohnen, "Euler/Lagrange calculations of turbulent sprays: the effect of droplet collisions and coalescence" *Atomization and Sprays,* vol 10, pp 47-81, 2000.

[4] G. Wigley, G. Pitcher, "PDA analysys of a poly-disperse GDI fuel spray with dropsize class discrimination", ILASS, Zurich, Switzeland, September 2001.

[5] J. Qian, C.K. Law. "Regimes of coalescence and separation in droplet collision". *Journal of Fluid Mechanics*, Vol 331, pp.59-80, 1997.

[6] S. Blei, C.A. Ho, M. Sommerfeld. "A stochastic droplet collision model with consideration of impact efficiency". ILASS 2002, Zaragoza, Spain, September 2002.